

MATHEMATICAL SIMULATION OF HEAT TRANSFER AND CHEMICAL REACTION IN A SWIRLING FLOW OF EQUILIBRIUM-DISSOCIATING GAS

O. V. Matvienko^{a,b} and P. S. Martynov^a

UDC 533.656:662.969+536.46

Results of investigations of the heat transfer in the swirling turbulent flow of dinitrogen tetroxide in a cylindrical channel are presented. The equilibrium stage of the dissociation reaction $N_2O_4 \rightleftharpoons 2NO_2$ was considered. It was established that the mass fraction of N_2O_4 in its swirling flow is smaller than that in the analogous forward flow at one and the same distance from the input cross section of the channel. In the case where the flow of dinitrogen tetroxide is strongly swirled, its intense heating in the zone of reverse flows near the channel inlet causes it to dissociate. It is shown that an increase in the swirling of a gas flow intensifies the heat transfer in it with increase in its Nusselt number.

Keywords: heat transfer, chemical reaction, dissociation, boundary layer, swirling flow, computational fluid dynamics.

Introduction. The study of the heat transfer in liquid and gas flows is of importance for different technologies. Solutions of problems on the heat transfer in the natural and forced convection flows of fluids in pipes and technological apparatus operating under different conditions are presented in [1, 2].

The study of the heat transfer in swirling flows takes on great significance because these flows are of frequent occurrence in practice. A swirling flow in a channel has its specific features differing it from the analogous forward flow [3]. A swirling flow is characterized by the commensurable axial, radial, and tangential velocities, the longitudinal and transverse pressure gradients, the large gradients of the axial velocity in the longitudinal and transverse directions, the intensive turbulent pulsations, and the active and conservative actions of the centrifugal forces in it on its turbulence.

Results of experimental and theoretical investigations of swirling flows and the heat and mass transfer in them are presented in [4, 5]. Experimental investigations on the heat transfer in internal swirling flows are described in great detail in [6–8]. The results of these investigations show that a local swirling of a fluid flow in a channel intensifies the heat transfer in it, with the result that its heat transfer coefficient changes sharply along the channel length [5]. The structure of the fluid flow in the immediate vicinity from a swirler in a channel and the heat transfer in it are determined by the method of the initial swirling of the fluid flow and by its intensity. At a distance from the inlet of the channel $x > (0.66\Phi_* + 0.44)d Re^{0.25}$, the heat transfer in the fluid flow and its structure are determined by only the intensity of swirling of the flow [5].

The heat transfer in the fluid flow in a pipe with $L/d \leq 100$, swirled by an axial vane swirler with a swirling angle constant along its height, was investigated fairly comprehensively in [9]. The twist φ of the vanes of the swirler was changed from 50 to 78° , and the relative diameter of its central body was $\bar{d}_0 = 0.65\text{--}0.83$. The experimental data obtained for the Reynolds numbers of the fluid flow $10^5 < Re < 10^7$ were generalized by the equation

$$Nu = 0.026(1 + \tan \varphi_{in})^{0.77} \exp(0.42\bar{d}_0^3 \Phi Re^{0.8}), \quad (1)$$

where $\Phi = (u_{max}/u_{max,in})^{0.8}$ is the parameter accounting for the change in the maximum axial velocity of the fluid flow along the length of the pipe. As the determining size of the swirling fluid flow at a certain cross section of the pipe, the distance from this cross section to the swirler x was used, and the determining temperature of the problem was the average temperature of the fluid flow at the indicated cross section T_{av} . The Reynolds number of the fluid flow in the pipe was determined by its maximum axial velocity u_{max} at cross section x . At $\varphi_{in} = 0$, expression (1) changes to the equation for the axial flow downstream of the bluff body in the pipe.

^aNational Research Tomsk State University, 36 Lenin Ave., Tomsk, 634050, Russia; ^bTomsk State University of Architecture and Building, 2 Solyanaya Sq., Tomsk, 634003, Russia; email: matvolegv@mail.ru. Translated from Inzhenerno-Fizicheskii Zhurnal, Vol. 95, No. 2, pp. 435–447, March–April, 2022. Original article submitted October 4, 2020.

The local heat transfer in the air flow in a pipe of length equal to its 12 diameters, swirled by an axial vane swirler with a central body of radius $\bar{r}_0 = 0.47$, was investigated in [4], and the following equation has been obtained for $3 \cdot 10^4 < \text{Re} < 1.5 \cdot 10^6$ and $15^\circ < \varphi_{\text{in}} < 60^\circ$:

$$\text{Nu}_x = 0.029 \text{Re}^{0.8} \text{Pr}^{0.4} \varepsilon_t \varepsilon_{\text{Nu}}, \quad (2)$$

where $\varepsilon_t = (2/(1 + \sqrt{T_w/\bar{T}}))^{1.6}$ is the nonisothermality function, and the function $\varepsilon_{\text{Nu}} = 1 + 0.44\Phi_*^{0.78}$ characterizes the influence of the swirling of the flow on the local heat transfer in it (here, Φ_* represents the current value of the Heeger–Baer integral swirling parameter).

The investigations of the heat transfer in the swirling fluid flow in a channel, performed in [10, 11], have shown that the heat transfer to the wall of the channel in its initial region increases with increase in the swirling of the flow, and the heat transfer at a large distance from the channel inlet is decreases this case. In the case of swirling of a fluid flow in a channel with a volumetric heat source of constant intensity, the heat transfer in the fluid flow decreases with increase in the swirling of the flow throughout its region.

To date a large number of experimental data on the heat transfer in the swirling flows of chemically inert fluids in channels has been accumulated, and numerous correlations have been proposed for concrete swirlers and flow conditions. However, the problems on the heat transfer in swirling flows of reacting fluids are as yet imperfectly understood and call for further complex investigations [12].

The study of the heat transfer in chemically reacting fluids is closely related to the problems on optimization of chemical technologies [13–20]. It is known that the use of reacting endothermic media for the heat carriers in different apparatus makes it possible to substantially increase the heat transfer in them compared to the heat transfer provided by inert heat carriers [21–23]. In [24, 25], calculation-theoretical investigations of the properties of a number of dissociating substances have been performed, and it was proposed for the first time to use dinitrogen tetroxide (N_2O_4) for the heat-transfer agent in an atomic power plant (APP) with a fast reactor. The experimental and theoretical investigations of the thermophysical properties of N_2O_4 , performed in [26, 27], have shown that this substance can be used to advantage in the nuclear power engineering. In [15, 28, 29], the heat transfer in flows of N_2O_4 was investigated, and relations for calculating the heat transfer in such flows with a chemical reaction have been proposed. It was shown that the use of N_2O_4 for the heat-transfer agent in an APP with a gas-cooled fast reactor makes it possible to simplify the design of the APP compared to that of analogous APPs operating with other heat-transfer agents [30–32].

The reaction of dissociation of dinitrogen tetroxide proceeds in the two stages: $\text{N}_2\text{O}_4 \rightleftharpoons 2\text{NO}_2 \rightleftharpoons 2\text{NO} + \text{O}_2$. In the case where N_2O_4 is heated, the first stage of its dissociation reaction proceeds rapidly and can be considered as equilibrium [33, 34], and the second stage of this reaction proceeds with a finite rate. The heat transfer processes taking place under the indicated conditions can be considered separately for each of the dissociation reaction stages [35].

The aim of the present work is numerical investigation of the influence of the swirling of the flow of an equilibrium dissociating gas (dinitrogen tetroxide) in a cylindrical channel on the heat transfer in it.

Mathematical Model. The structure of the axisymmetric flow of dinitrogen tetroxide in a cylindrical channel was defined by the two-dimensional Reynolds equations for the time-averaged axial, radial, and tangential velocities of the gas flow and its pressure p [36]:

$$\frac{\partial \rho u}{\partial x} + \frac{1}{r} \frac{\partial \rho v r}{\partial x} = 0, \quad (3)$$

$$\frac{\partial \rho u^2}{\partial x} + \frac{1}{r} \frac{\partial \rho u v r}{\partial r} = -\frac{\partial p}{\partial x} + \frac{\partial}{\partial x} \left[\mu_{\text{eff}} \left(2 \frac{\partial u}{\partial x} - \frac{2}{3} \left(\frac{\partial u}{\partial x} + \frac{1}{r} \frac{\partial v r}{\partial r} \right) \right) \right] + \frac{1}{r} \frac{\partial}{\partial r} \left[\mu_{\text{eff}} r \left(\frac{\partial u}{\partial r} + \frac{\partial v}{\partial x} \right) \right], \quad (4)$$

$$\frac{\partial \rho u v}{\partial x} + \frac{1}{r} \frac{\partial \rho v^2 r}{\partial r} = -\frac{\partial p}{\partial r} + \frac{\partial}{\partial x} \left[\mu_{\text{eff}} \left(\frac{\partial v}{\partial x} + \frac{\partial u}{\partial r} \right) \right] + \frac{1}{r} \frac{\partial}{\partial r} \left[\mu_{\text{eff}} r \left(2 \frac{\partial v}{\partial r} - \frac{2}{3} \left(\frac{\partial u}{\partial x} + \frac{1}{r} \frac{\partial v r}{\partial r} \right) \right) \right] - 2 \frac{\mu_{\text{eff}} v}{r^2} + \frac{\rho w^2}{r}, \quad (5)$$

$$\frac{\partial \rho u w}{\partial x} + \frac{1}{r} \frac{\partial \rho v w r}{\partial r} = \frac{\partial}{\partial x} \left[\mu_{\text{eff}} \frac{\partial w}{\partial x} \right] + \frac{1}{r^2} \frac{\partial}{\partial r} \left[\frac{\mu_{\text{eff}}}{\sigma_{r\varphi}} r^3 \frac{\partial}{\partial r} \left(\frac{w}{r} \right) \right] - \frac{\rho v w}{r}. \quad (6)$$

The turbulence characteristics of the gas flow were investigated using the Menter combined k - ε model of turbulence [38, 37]:

$$\frac{\partial \rho u k}{\partial x} + \frac{1}{r} \frac{\partial \rho v k r}{\partial r} = \frac{\partial}{\partial x} \left[(\mu + \sigma_k \mu_t) \frac{\partial k}{\partial x} \right] + \frac{1}{r} \frac{\partial}{\partial r} \left[(\mu + \sigma_k \mu_t) r \frac{\partial k}{\partial r} \right] + F_2 \tilde{G} - C_{\mu} \rho \omega k, \quad (7)$$

$$\begin{aligned} \frac{\partial \rho u \omega}{\partial x} + \frac{1}{r} \frac{\partial \rho v \omega r}{\partial r} &= \frac{\partial}{\partial x} \left[(\mu + \sigma_{\omega} \mu_t) \frac{\partial \omega}{\partial x} \right] + \frac{1}{r} \frac{\partial}{\partial r} \left[(\mu + \sigma_{\omega} \mu_t) r \frac{\partial \omega}{\partial r} \right] \\ &+ \left(\frac{C_{\beta}}{C_{\mu}} - \frac{\sigma_{\omega}}{\sqrt{C_{\mu}}} \kappa^2 \right) \frac{\rho}{\mu_t} F_2 \tilde{G} - C_{\beta} \rho \omega^2 + (1 - F_1) C_{k\omega}. \end{aligned} \quad (8)$$

The intensity of the shear deformations of the gas flow (the second invariant of the rate-of-strain deviator) was determined by the expression

$$G = 2 \left[\left(\frac{\partial u}{\partial x} \right)^2 + \left(\frac{\partial v}{\partial r} \right)^2 + \left(\frac{v}{r} \right)^2 \right] + \left(\frac{\partial u}{\partial r} + \frac{\partial v}{\partial x} \right)^2 + \left(\frac{\partial w}{\partial x} \right)^2 + \left(r \frac{\partial w/r}{\partial r} \right)^2.$$

The limiter $\tilde{G} = \min [\mu_t G, 20 C_{\mu} \rho \omega k]$ was introduced into Eq. (7) for calculating the energy of turbulence generation. The last term in Eq. (8) defines the crossed diffusion $C_{k\omega} = 2 \rho \sigma_{\omega} \omega^{-1} \left(\frac{\partial k}{\partial x} \frac{\partial \omega}{\partial x} + \frac{\partial k}{\partial r} \frac{\partial \omega}{\partial r} \right)$. The function of mixing of the gas in the channel and its argument were determined by the relations

$$F_1 = \tanh (F_3^4), \quad F_3 = \min \left[\max \left(\frac{\sqrt{k}}{C_{\mu} \omega d_w}, \frac{500 \mu}{\rho d_w^2 \omega} \right), \frac{4 \rho \sigma_{\omega} k}{\max [C_{k\omega}, 10^{-20}] d_w^2} \right].$$

The above-described model of turbulence of a gas flow in a channel was modified by introduction, into it, the correction function $F_2 = \max [\min [f_{\text{rot}}, 1.25], 0]$ accounting for the swirling of the flow [39]. This function was calculated using the dependences [40]

$$f_{\text{rot}} = 2 \xi^* \left(\frac{1 + C_{\xi 1}}{1 + \xi^*} \right) (1 - C_{\xi 3} \arctan (C_{\xi 2} \tilde{\xi})) - C_{\xi 1}, \quad \tilde{\xi} = 2 \frac{\Omega_{jk} \dot{\xi}_{jk}}{\Omega F_4^3} \left(\frac{D \dot{\xi}_{ij}}{Dt} \right), \quad \xi^* = \frac{\sqrt{G}}{\Omega^2},$$

$$F_4 = \sqrt{\max (G, C_{\mu} \omega^2)}, \quad \Omega = \sqrt{\frac{1}{2} \left[\left(\frac{\partial v}{\partial x} - \frac{\partial u}{\partial r} \right)^2 + \left(\frac{\partial w}{\partial x} \right)^2 + \left(\frac{1}{r} \frac{\partial r w}{\partial r} \right)^2 \right]}.$$

The components of the strain-rate and vorticity tensors of the gas flow were determined by the relations

$$\dot{\varepsilon}_{xr} = \dot{\varepsilon}_{rx} = \frac{1}{2} \left(\frac{\partial v}{\partial x} + \frac{\partial u}{\partial r} \right), \quad \dot{\varepsilon}_{x\varphi} = \dot{\varepsilon}_{\varphi x} = \frac{1}{2} \left(\frac{\partial w}{\partial x} \right), \quad \dot{\varepsilon}_{r\varphi} = \dot{\varepsilon}_{\varphi r} = \frac{1}{2} \left(r \frac{\partial w/r}{\partial r} \right),$$

$$\dot{\varepsilon}_{xx} = \frac{\partial u}{\partial x}, \quad \dot{\varepsilon}_{rr} = \frac{\partial v}{\partial r}, \quad \dot{\varepsilon}_{\varphi\varphi} = \frac{v}{r},$$

$$\Omega_{xr} = -\Omega_{rx} = -\frac{1}{2} \left(\frac{\partial v}{\partial x} - \frac{\partial u}{\partial r} \right), \quad \Omega_{x\varphi} = -\Omega_{\varphi x} = -\frac{1}{2} \left(\frac{\partial w}{\partial x} \right), \quad \Omega_{r\varphi} = -\Omega_{\varphi r} = -\frac{1}{2} \left(\frac{1}{r} \frac{\partial r w}{\partial r} \right),$$

$$\Omega_{xx} = 0, \quad \Omega_{rr} = 0, \quad \Omega_{\varphi\varphi} = 0.$$

For a stationary axisymmetric gas flow, the substantive derivative of the strain-rate tensor components has the form $\frac{D\dot{\varepsilon}_{ij}}{Dt} = u \frac{\partial \dot{\varepsilon}_{ij}}{\partial x} + v \frac{\partial \dot{\varepsilon}_{ij}}{\partial r}$. The effective viscosity of the gas flow was determined as the sum of its molecular (μ) and turbulent (μ_t) viscosities: $\mu_{\text{eff}} = \mu + \mu_t$. The turbulent viscosity of the gas flow was determined by the known values of the coefficients k and ω in the SST model with the use of the expression based on the Bradshaw hypothesis [40] for the proportionality of the shear stress of the gas flow in the boundary layer near the wall of the channel to the energy of the turbulent flow pulsations: $\mu_t = \min \left[\frac{\rho k}{\omega}, \frac{\gamma \rho k}{F_5 G} \right]$. The empirical function F_7 was calculated by the formula

$$F_5 = \tanh(F_6^2), \quad F_6 = \max \left[2 \frac{\sqrt{k}}{C_\mu \omega d_w}, \frac{500\mu}{d_w^2 \rho \omega} \right].$$

The empirical constants were expressed in terms of the corresponding constants of the k - ε and k - ω models with the use of the function F_1 :

$$\sigma_k = F_1 \sigma_{k1} + (1 - F_1) \sigma_{k2}, \quad \sigma_\omega = F_1 \sigma_{\omega1} + (1 - F_1) \sigma_{\omega2}, \quad C_\beta = F_1 C_{\beta1} + (1 - F_1) C_{\beta2}.$$

Here, the subscripts 1 and 2 are related, respectively, to the constants of the k - ε and k - ω models: $\sigma_{k1} = 0.85$, $\sigma_{\omega1} = 0.5$, $C_{\beta1} = 0.075$, $\sigma_{k2} = 1$, $\sigma_{\omega2} = 0.856$, and $C_{\beta2} = 0.0828$. The values of the other constants were selected in accordance with the recommendations given in [37–39]: $\gamma = 0.31$, $C_\mu = 0.09$, $C_{\xi1} = 1$, $C_{\xi2} = 2$, $C_{\xi3} = 1$, and $\kappa = 0.41$.

The heat transfer in the gas flow in the channel was simulated using the equation for the heat conductivity of the gas with regard for the chemical reaction proceeding in it [15, 29]:

$$C_p \left(\frac{\partial \rho u T}{\partial x} + \frac{1}{r} \frac{\partial \rho v r T}{\partial r} \right) = \frac{\partial}{\partial x} \left[\lambda_{\text{eff}} \frac{\partial T}{\partial x} \right] + \frac{1}{r} \frac{\partial}{\partial r} \left[\lambda_{\text{eff}} r \frac{\partial T}{\partial r} \right] - Q \Psi. \quad (9)$$

The effective thermal diffusivity of the gas was determined by the relation $\lambda_{\text{eff}} = \frac{\mu}{\text{Pr}} + \frac{\mu_t}{\text{Pr}_t}$. It was assumed that the Prandtl turbulence number is equal to $\text{Pr}_t = C_p \mu_t / \lambda_t = 0.7$, and the heat released in the chemical reaction proceeding in the gas flow comprises $Q = -624$ kJ/kg [41]. The rate of an equilibrium chemical reaction was determined by the expression

$$\Psi = \rho \left(u \frac{\partial M_{\text{N}_2\text{O}_4}}{\partial x} + v \frac{\partial M_{\text{N}_2\text{O}_4}}{\partial r} \right). \quad (10)$$

The concentration of dinitrogen tetroxide in its flow with an equilibrium chemical reaction was determined by the equality of the rates of the direct and inverse chemical reactions in the flow:

$$k_+ \left(\frac{\rho M_{\text{NO}_2}}{W_{\text{NO}_2}} \right)^2 - k_- \left(\frac{\rho M_{\text{N}_2\text{O}_4}}{W_{\text{N}_2\text{O}_4}} \right) = 0, \quad (11)$$

where $M_{\text{N}_2\text{O}_4}$, $M_{\text{NO}_2} = 1 - M_{\text{N}_2\text{O}_4}$, $W_{\text{N}_2\text{O}_4}$, and W_{NO_2} are the mass fractions and molar masses of dinitrogen tetroxide and nitrogen oxide (NO_2) in the gas flow, respectively. The equilibrium constant of the chemical reaction, expressed in terms of the mass fractions of the reagents, was determined by the expression [42]

$$K_c = \frac{k_-}{k_+} = \frac{K_p}{R_g T}. \quad (12)$$

The temperature dependence of this constant was defined by the Van't Hoff isobar equation

$$\left(\frac{d \ln K_p}{dT} \right)_p = \frac{Q}{R_g T^2}. \quad (13)$$

Integration of (13) gives the dependence of K_p on the temperature

$$K_p = K_{p0} \exp\left(\frac{QT_0T}{R_g(T_0 - T)}\right), \quad (14)$$

where $K_{p0} = 14.29$ KPa at $T_0 = 298$ K. The density of the gas ρ was determined by the equation for its state

$$\rho = \frac{p}{R_g T} \left(\frac{M}{W_{N_2O_4}} + \frac{1 - M}{W_{NO_2}} \right)^{-1}. \quad (15)$$

The velocity, temperature, and turbulence parameters of the gas flow at the inlet of the channel were determined by the relations

$$u = u_{in}, \quad v = 0, \quad w = Ro u_{in} \left(\frac{r}{R} \right), \quad k = Tu(u_{in}^2 + w_{in}^2), \quad \omega = C_\omega k_{in}^{1/2} / R, \quad T = T_{in},$$

where $C_\omega = 5$, and Ro determines the angular velocity of the gas flow: $\dot{\phi} = Ro u_{in} / R$ [3, 43]. The boundary conditions at the outlet cross section of the channel ($x = L$) have the form

$$\frac{\partial u}{\partial x} = 0, \quad v = 0, \quad \frac{\partial w}{\partial x} = 0, \quad \frac{\partial k}{\partial x} = 0, \quad \frac{\partial \omega}{\partial x} = 0, \quad \frac{\partial T}{\partial x} = 0.$$

At the axis of the channel ($r = 0$), the symmetry conditions

$$\frac{\partial u}{\partial r} = 0, \quad v = 0, \quad w = 0, \quad \frac{\partial k}{\partial r} = 0, \quad \frac{\partial \omega}{\partial r} = 0, \quad \frac{\partial T}{\partial r} = 0$$

were set. It was assumed that the adhesion and ideal heat conduction conditions are fulfilled at the walls of the channel ($r = R$) and that the kinetic energy of turbulence at them is equal to zero:

$$r = R, \quad u = 0, \quad v = 0, \quad w = 0, \quad k = 0, \quad T = T_w.$$

The frequency of turbulent pulsations of the gas flow was determined at the finite-difference mesh node, nearest to the channel wall, with coordinate r_{nw} by the formula

$$\omega_{nw} = C_1 \frac{\mu}{\rho(R - r_{nw})^2},$$

where $C_1 = 80$.

Method of Solution of the Problem. Equations (3)–(9) were solved numerically by the method of finite volumes [44] on a staggered mesh whose nodes for the axial and radial velocity components of the gas flow in the channel were positioned at the center of the faces of the control volumes of the scalar quantities. This mesh had 2000 nodes in the axial direction and 1700 nodes in the radial direction. Near the walls of the channel and in the regions of the gas flow with large velocity and concentration gradients, the mesh was bunched.

The equation of continuity of the gas flow in the channel was solved using the SIMPLEC algorithm [45]. Iterations were considered as converged when the quadratic mean error in determining all the variables was not larger than 1%. For estimating the accuracy of calculations, they were tested on a sequence of bunching meshes. These tests have shown that a decrease in the steps of the base mesh along the axial and radial coordinates by two times leads to a change in the values of the main variables by no more than 1%.

Results of Mathematical Simulation. A numerical investigation of the influence of the swirling of the flow of an equilibrially dissociating gas (dinitrogen tetroxide) in a cylindrical channel on the structure of this flow and the heat transfer in it has been performed. Figure 1 shows radial distributions of the tangential velocity of the gas flow in the channel, calculated for different Rossby numbers. In the case of weak or moderate swirling of the gas in the channel its flow at the axis of the channel and in its peripheral regions is quasi-solid with a linear tangential-velocity profile. When the gas in the

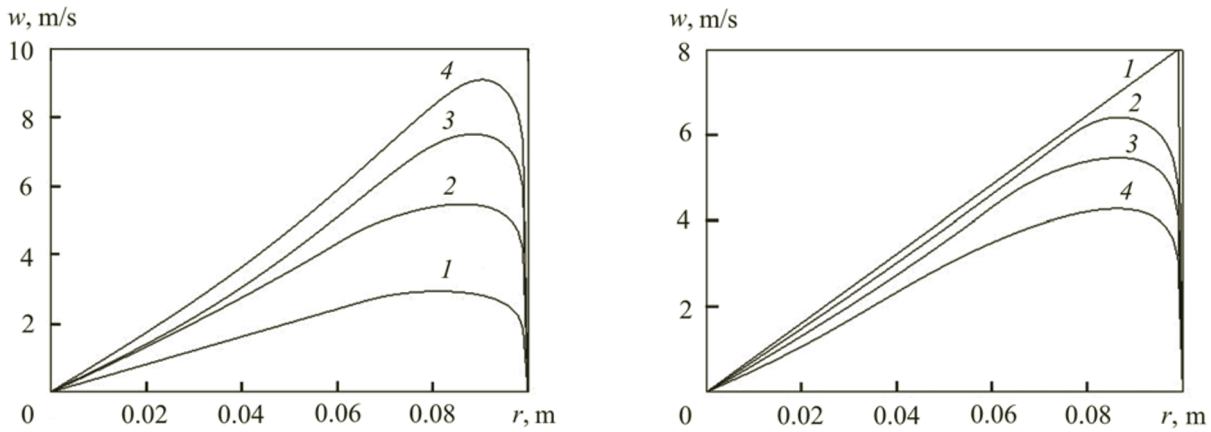


Fig. 1. Radial distribution of the tangential velocity of the chemically reacting gas flow in a cylindrical channel at $u_{in} = 10$ m/s, $T_{in} = 300$ K, $T_w = 600$ K, and $x = 0.5$ m: 1) $Ro = 4$; 2) 8; 3) 12; 4) 16.

Fig. 2. Radial distribution of the tangential velocity of the chemically reacting gas flow in the channel at $u_{in} = 1$ m/s, $Ro = 8$, $T_{in} = 300$ K, and $T_w = 600$ K: 1) $x = 0$ m; 2) 0.2; 3) 0.4; 4) 0.8.

channel is swirled strongly, the distribution of the tangential velocity of the gas flow along the channel axis is not linear, which points to the fact that in the gas flow there appear shear stresses determined by the relation $\sigma_{r\varphi} = \mu_{eff} \left(\frac{\partial w}{\partial r} - \frac{w}{r} \right)$. As the swirling of the gas flow decreases with distance from the inlet of the channel, the profile of its tangential velocity becomes linear. Near the wall of the channel there arises a boundary layer in which the tangential velocity of the gas flow is decreased. In this case, the tangential velocity of the gas flow at the wall of the channel is equal to zero, which is explained by the adhesion of the gas to the channel wall because of its viscous interaction with this wall. As the swirling of the gas flow at the inlet of the channel increases (with increase in the Rossby number) the tangential velocity of the gas flow in the channel increases throughout its cross section.

The radial distributions of the tangential velocity of the gas flow in the channel at its different cross sections are shown in Fig. 2. The swirling of the gas at the inlet of the channel was simulated on the assumption that its rotation is quasi-solid with the result that the linear profile of the tangential velocity of the gas flow at the channel inlet has been obtained. The tangential flow velocity decreases downstream because of the action of the viscous forces. As the swirling of the gas in the channel decreases, the radial coordinate of the gas flow with a maximum tangential velocity shifts to the central region of the channel. The results of calculations show that, at a distance $x/R = 0.88Re^{0.25}Ro$ from the inlet of the channel, the swirling of the gas flow degenerates, and it becomes forward.

A weak swirling of the gas in the channel ($Ro < 4$) insignificantly decreases the velocity of its flow at the axis of the channel and in its central zones. In the case where the gas in the channel is swirled strongly ($Ro > 4$), the velocity of the gas flow at the wall of the channel is increased because of the movement of the gas from the central part of the channel to its wall. Near the wall of the channel there arises a zone in which the radial distribution of the axial velocity of the gas flow has a local maximum, and the radial distribution of the axial velocity of the gas flow near the axis of the channel has a minimum (Fig. 3).

In the case where the gas in the channel is swirled strongly ($Ro > 10$), the depth of the dip of the velocity curve of the gas flow in the neighborhood of the channel axis increases, which points to the formation of a reverse flow zone.

Figure 4 shows the temperature isolines of the flow of a chemically inert gas in a cylindrical channel, calculated for different degrees of swirling of this flow. It is seen that, near the wall of the channel there is a region where the temperature of the gas changes sharply. The temperature in the core of the gas flow in the initial region of the channel takes constant values equal to the initial temperature of the gas flow. In this region of the channel there is no heat exchange between the gas and the channel wall. As the distance from the inlet cross section of the channel increases, the near-wall layers of the gas

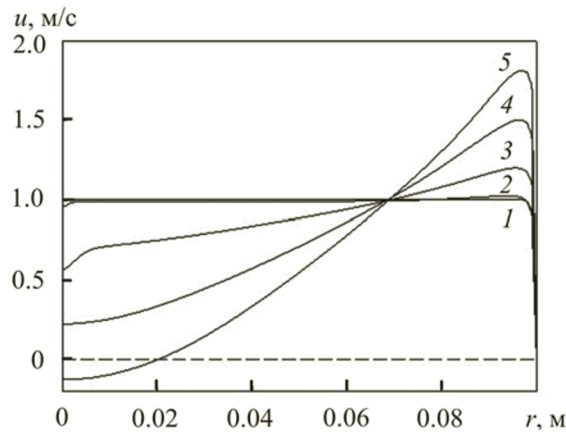


Fig. 3. Radial distribution of the axial velocity of the chemically reacting gas flow in the channel at $u_{in} = 1$ m/s, $T_{in} = 300$ K, $T_w = 600$ K, and $x = 0.5$ m: 1) $Ro = 0$; 2) 4; 3) 8; 4) 12; 5) 16.

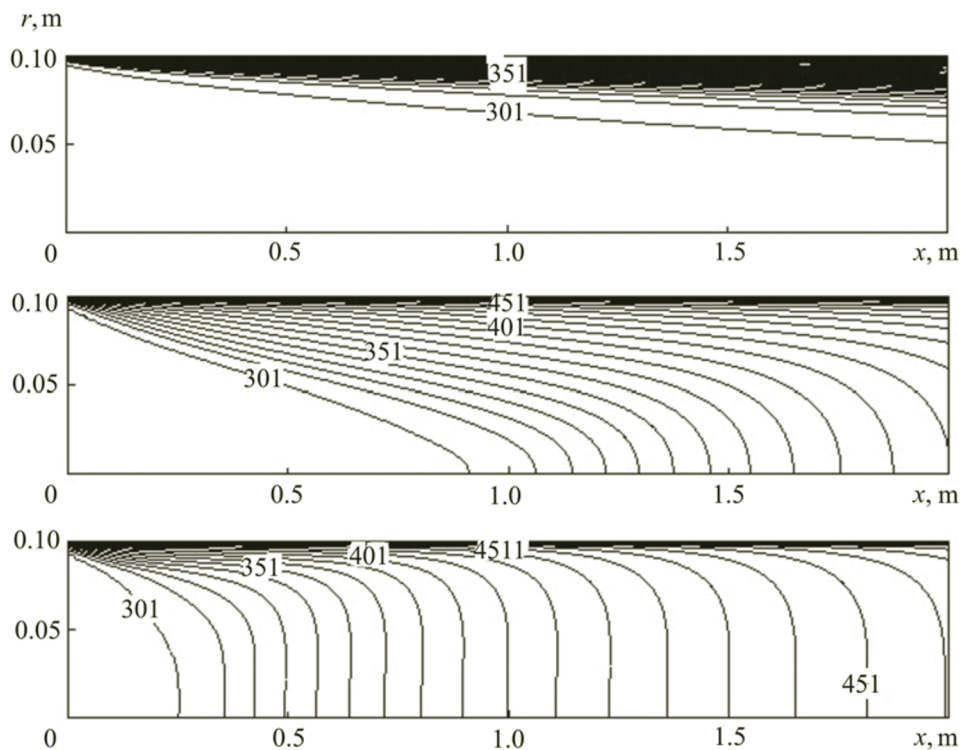


Fig. 4. Isotherms of the chemically inert gas flow in the channel at $u_{in} = 1$ m/s, $T_{in} = 300$ K, $T_w = 600$ K: a) $Ro = 0$; b) 8; c) 16.

are heated and, therefore, along with the dynamic boundary layer, a temperature boundary layer is formed in the gas flow. The thickness of the temperature boundary layer increases with increase in the distance from the inlet of the channel and, at a large distance from it, this layer reaches the axis of the channel. However, the heat exchange process is not completed at this point. The temperature of the gas will change downstream as long as it is equal to the temperature of the channel wall.

The temperature fields of a forward gas flow in a cylindrical channel and of a weakly swirled one ($0 < Ro < 2$) are similar. An increase in the intensity of swirling of the gas flow in the channel (with increase in its Rossby number) leads to an increase in the thickness of the temperature boundary layer of the flow. At $Ro > 4$, the boundary layer occupies the whole region of the flow at a fairly close distance from the inlet of the channel. A further increase in the swirling of the gas flow

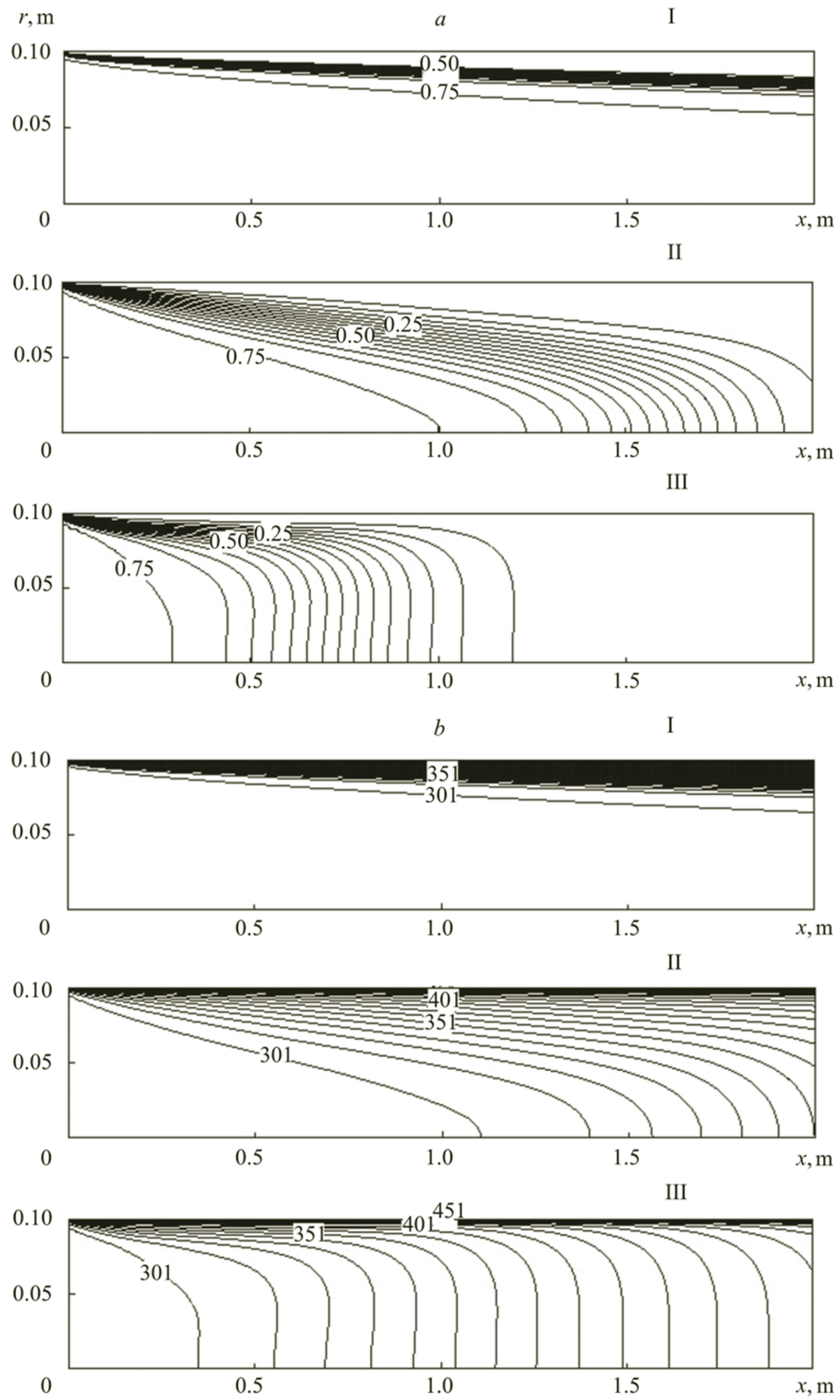


Fig. 5. Isolines of the mass fractions of the chemically reacting gas (a) and isotherms (b) in the flow of this gas in the channel at $u_{in} = 1$ m/s, $T_{in} = 300$ K, $T_w = 600$ K, and $Ro = 0$ (I), 8 (II), and 16 (III).

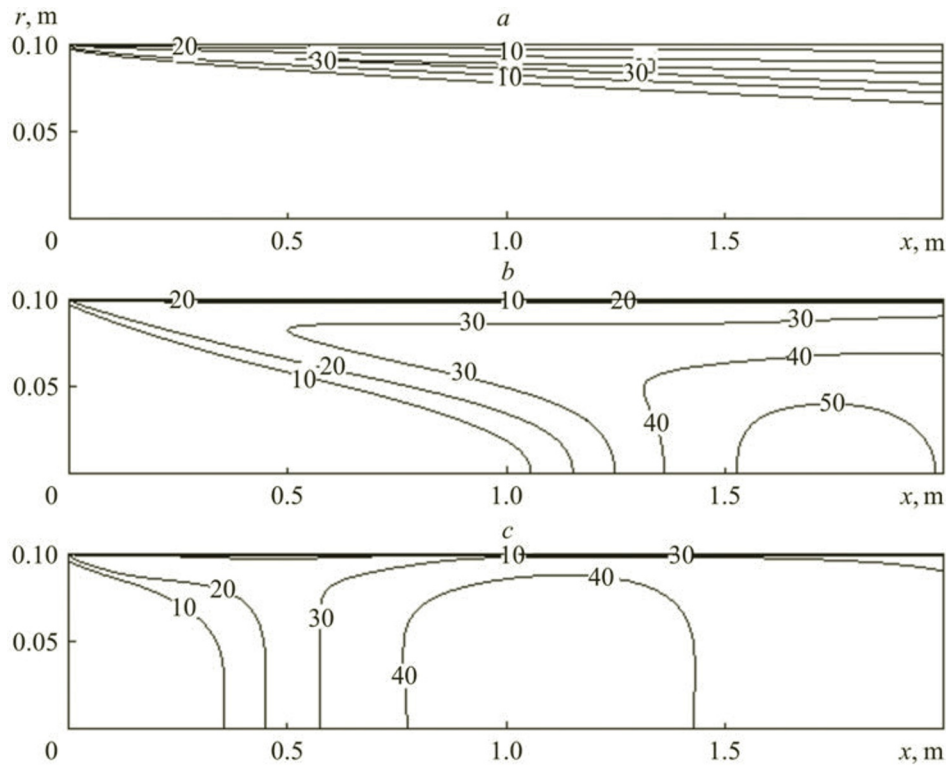


Fig. 6. Temperature differences in the chemically inert and reacting gas flows at $u_{in} = 1$ m/s, $T_{in} = 300$ K, $T_w = 600$ K, and $Ro = 0$ (a), 8 (b), and 16 (c).

causes the coordinate of the joint of the boundary layers in it to shift to the inlet cross section of the channel. When the gas is swirled strongly, in the channel there arise circulating flows, due to which, the heated gas masses at the cross sections of the channel, located at large distances from its inlet, move upstream and aid in the heating of the gas flow region in which the temperature boundary layer reaches the axis of the channel, with the result that the length of this region decreases rapidly.

The heating of the near-wall layers of the flow of dinitrogen tetroxide in the channel leads to a shift of its chemical equilibrium to the side of formation of dinitrogen dioxide. As a result, the concentration of dinitrogen tetroxide in the near-wall region of the flow decreases substantially, and a concentration boundary layer is formed in it (Fig. 5a). The formation of this layer in the chemically reacting gas flow is analogous to the formation of a temperature boundary layer in it. The thickness of the concentration boundary layer of the gas in the channel increases downstream. An increase in the swirling of the gas in the channel leads to an increase not only in the temperature of the gas flow near the wall of the channel, but also in the temperature of the gas flow near the channel axis. Because of this, at one and the same distance from the inlet of the channel, the mass fraction of N_2O_4 in its swirling flow is smaller than that in the forward one. It should be noted that, in the case where the flow of dinitrogen tetroxide is strongly swirled, the intensive heating of it due to its circulation in the zone of reverse flows leads to the decomposition of N_2O_4 at a small distance from the inlet of the channel. The influence of the swirling of the flow of the equilibrium dissociating gas on the formation of the temperature field in it is shown in Fig. 5b. It is seen from this figure that the main mechanisms of the formation of temperature fields in the chemically inert and chemically reacting gases are identical. However, since the chemical transformation of a gas is an endothermic process, the temperature of the near-wall layer in the chemically reacting gas flow is lower and the thickness of its temperature boundary layer is smaller than those of the inert gas flow.

The influence of the chemical reaction in the flow of dinitrogen tetroxide in the channel on the temperature field in it depending on its swirling is shown in Fig. 6. In the initial region of the channel, in which the channel wall exerts no heat action on the gas flow in it or exerts a minimum action on the gas flow, the temperature of the gas is close to its temperature at the inlet cross section of the channel. Because of this, in the indicated region of the channel there is no dissociation of the heat-transfer agent, and the temperature of the chemically reacting gas flow is equal to the temperature of the inert gas flow. As the flow of dinitrogen tetroxide is heated and the reaction of its transformation intensifies, the temperature difference in the gas flow increases. The chemical reaction zones in the forward flow of N_2O_4 and in its weakly swirled flow ($Ro < 2$)

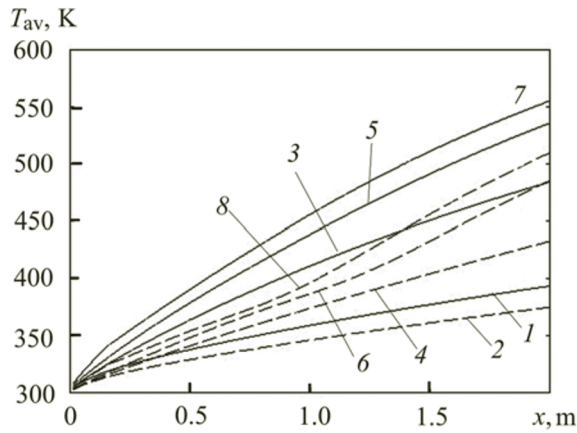


Fig. 7. Change in the average temperature of the chemically reacting gas (full lines) and the reacting gas flow (dashed lines) in the channel with distance from its inlet at $u_{in} = 1$ m/s, $T_{in} = 300$ K, $T_w = 600$ K, and $Ro = 0$ (1, 2), 4 (3, 4), 8 (5, 6), and 12 (7, 8).

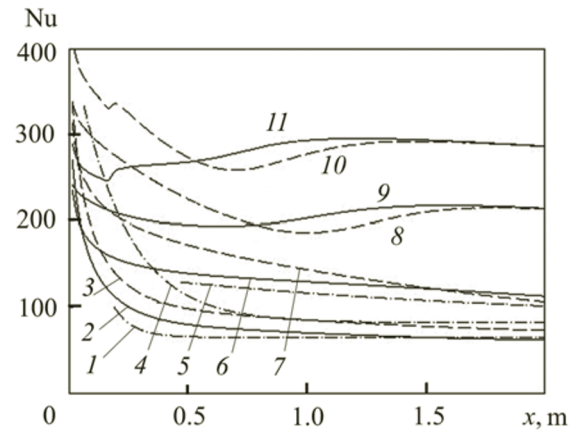


Fig. 8. Change in the Nusselt number of the chemically inert gas flow (full lines) and the reacting gas flow (dashed lines) in the channel with distance from its inlet at $p_{in} = 1$ MPa, $u_{in} = 1$ m/s, $T_{in} = 300$ K, $T_w = 600$ K, and $Ro = 0$ (1–4), 4 (5–7), 8 (8, 9), and 12 (10, 11): 1) data of [1]; 4) data of [52]; data of [5].

are located near the wall of the channel. Because of this, ΔT takes maximum value at the channel wall. With increase in the swirling of the gas flow and with heating of its inner layers, the region of maximum values of ΔT shifts to the axis of the channel. As the dissociation of dinitrogen tetroxide is completed downstream, the difference between the temperatures of the inert and reacting gases decreases.

Figure 7 presents distributions of the average temperature of the inert and chemically reacting gas flows, determined as $T_{av} = \frac{\int_0^R \rho u T r dr}{\int_0^R \rho u r dr}$, downstream from the inlet cross section of the channel. This temperature increases with thermal stabilization of a gas flow and with its swirling intensifying the convective heat transfer in it. Due to the endothermic reaction proceeding in the chemically reacting gas, the average temperature of its flow is lower than that of the inert gas. The bends of curves 6 and 8 point to the completion of the dissociation of N_2O_4 and the beginning of the inert heating of NO_2 .

The changes in the Nusselt numbers of the chemically inert gas and the equilibrium dissociating gas downstream from the inlet of the channel is shown in Fig. 8. It is seen that the results of calculations of this changes are in good agreement with the corresponding experimental data. The Nusselt number of a forward gas flow ($Ro = 0$) and of a weakly or moderately swirled one ($Ro < 6$) decreases monotonically downstream. This effect is explained by the fact that the temperature gradient in the indicated flows at the wall of the channel $\left. \frac{\partial T}{\partial r} \right|_{r=R}$ decreases with increase in the distance from the channel inlet more rapidly than the average temperature of these flows increases because the central part of them does not participate in the heat exchange. The Nusselt number of a gas flow decreases as long as the boundary heat layers in it close up. Then the both quantities decrease with equal rates, and the local heat transfer coefficient takes a constant value.

As the axial velocity of a swirling gas flow in the peripheral region of the channel increases, the heated near-wall layers of the flow move rapidly downstream, and they have no time to transfer their heat to the inner layers of the flow, with the result that the heat flow in the channel increases. An increase in the rate of the near-wall flow at any cross section of the channel leads to an increase in the average temperature at this cross section. The last-mentioned factor is deciding in determining the influence of the swirling of the gas flow on the heat transfer in it. It is precisely an increase in T_{av} of the gas flow in the indicated region of the channel that leads to an increase in its Nusselt number determined by the relation

$$Nu = \frac{2R}{T_w - T_{av}} \left. \frac{\partial T}{\partial r} \right|_{r=R} \quad (16)$$

Thus, an increase in the Rossby number of a gas flow in a cylindrical channel causes the Nusselt number of the flow to increase throughout its region, and the largest heat transfer is realized in the region of the channel where the centrifugal forces predominate. The high velocity of movement of the gas in this region results in that the thickness of the boundary layer of its flow decreases and, therefore, the conditions of heat transfer in it become better. Because of this, an increase in the Rossby number of the gas flow in the indicated region of the channel leads to an increase in its length with increase in

both the local heat transfer and the integral one $\left(\overline{\text{Nu}} = \frac{1}{L} \int_0^L \text{Nu} \, dx \right)$ in it. As the swirling of the gas flow degenerates, its

Nusselt number takes values equal to those of the forward gas flow. In the case where the gas flow is swirled strongly, its Nusselt number changes downstream nonmonotonically. This effect was observed in experiments and was explained for the first time in [4, 5, 43]. The nonmonotonic change in the Nusselt number of a strongly swirled gas flow is explained by the complex influence of the swirling of the flow on the generation and dissipation of turbulence in it. The indicated influence in the region of the gas near the swirler in the channel is conservative in character. Therefore, the gas flow in this region is laminar, and it turbulizes downstream [4, 43]. In the process of formation of a boundary temperature layer in a swirling gas flow, its Nusselt number decreases and, at a large distance from the swirler, takes values equal to those of the forward gas flow. The heat transfer in the initial region of the flow of the equilibrium-dissociating gas in the channel is increased due to the heat generated in the intense endothermic reaction proceeding near the wall of the channel. After the dissociation of the heat-transfer agent is completed, it is inertially heated downstream, with the result that the temperature gradient at the wall of the channel decreases. Since the average temperature of the reacting gas flow is lower than that of the inert gas flow, in accordance with dependence (16), the Nusselt number of the reacting gas flow is smaller than that of the inert gas flow. On completion of the dissociation of the chemically reacting gas, the Nusselt number of its flow throughout the cross section of the channel, located at a large distance from its inlet, becomes equal to that of the inert gas flow. Note that, as the swirling of the gas flow in the channel increases, the contribution of the chemical reaction in it into its Nusselt number becomes more significant.

Conclusions. Our calculations have shown that an increase in the swirling of the flow of dinitrogen tetroxide in a cylindrical channel leads to an increase in the thickness of the boundary temperature layer in it and causes the joint of the boundary layers in the flow to shift to the outlet of the channel. In this case, both the temperature of the gas flow in the near-wall region of the channel and the temperature of the gas flow in its axial region increase. At a definite distance from the inlet cross section of the channel, the mass fraction of N_2O_4 in its swirling flow is smaller than that in the forward flow of this gas. In the case of strong swirling of the flow of dinitrogen tetroxide in the channel, the strong heating of it in the zone of reverse flows leads to the decomposition of N_2O_4 at a small distance from the inlet cross section of the channel. An increase in the swirling of the gas flow intensifies the heat transfer in it and leads to an increase in its Nusselt number. The Nusselt number of the forward gas flow ($\text{Ro} = 0$) in the channel as well as of a weakly or moderately swirled one ($\text{Ro} < 6$) decreases monotonically downstream, and the Nusselt number of the strongly swirled gas flow changes downstream nonmonotonically because of the complex action of the swirling of the flow on the generation and dissipation of turbulence in it. Near the swirler in the channel, this action is conservative in character and, therefore, the gas flow is laminar. At a larger distance from the swirler, the gas flow becomes turbulent, and the heat transfer in it increases.

NOTATION

C_p , heat capacity of the gas at a constant pressure, J/(kg·K); d_w , distance from a reference point to the nearest point at the wall of a channel, m; G , intensity of shear deformations, s^{-2} ; k_+ , rate of dimerization of NO_2 , $\text{m}^3/(\text{mole}\cdot\text{s})$; k_- , rate of dissociation of N_2O_4 , s^{-1} ; k , kinetic energy of turbulence, m^2/s^2 ; K_c and K_p , equilibrium constants of a chemical reaction expressed in terms of the molar concentrations and the partial pressures of the reagents, mole/m^3 , Pa; L , length of the channel, m; M , mass concentration; Nu, Pr, and Ro, Nusselt, Prandtl, and Rossby numbers; p , pressure Pa; Q , heat of a chemical reaction, J/kg; Re, mean-integral Reynolds number; r , radial coordinate, m; R , radius of the channel, m; R_g , universal gas constant, J/(mole·K); T_u , intensity of turbulence at the inlet of the channel; u , v , and w , axial, radial, and tangential velocities of a gas flow, m/w; W , molecular mass, kg/mole; x , axial coordinate, m; ε , rate of dissipation of turbulence energy, W/kg; λ , heat conductivity of the gas, W/(m·K); μ , dynamic viscosity of the gas, Pa·s; ρ , density of the gas, $\text{kg}/(\text{m}^3\cdot\text{s})$; $\sigma_{r\varphi}$, shear stresses, Pa; φ , swirling angle, deg; κ , Karman constant; Ψ , rate of an equilibrium chemical reaction, $\text{kg}/(\text{m}^3\cdot\text{s})$; ω , frequency of turbulent pulsations, s^{-1} . Subscripts: av, average; eff, effective; in, inlet; max, maximum; nw, near-wall; t, turbulent; w, wall.

REFERENCES

1. B. S. Petukhov and V. K. Shikov (Eds.), *Heat Exchanger Design Handbook* [Russian translation], Énergoatomizdat, Moscow (1987).
2. A. V. Luikov, *Heat and Mass Transfer* [in Russian], Énergiya, Moscow (1978).
3. A. K. Gupta, D. G. Lilley, and N. Syred, *Swirl Flows* [Russian translation], Mir, Moscow (1987).
4. V. K. Shchukin and A. A. Khalatov, *Heat and Mass Transfer and Hydrodynamics of Swirling Flows in Axisymmetric Channels* [in Russian], Mashinostroenie, Moscow (1982).
5. A. A. Khalatov, *Theory and Practice of Swirling Flows* [in Russian], Naukova Dumka, Kiev (1989).
6. I. V. Shevchuk and A. A. Khalatov, Heat transfer and hydrodynamics in channels rotating about their axis, *J. Eng. Phys. Thermophys.*, **70**, No. 3, Article number 511 (1997).
7. I. V. Shevchuk and A. A. Khalatov, Heat transfer and hydrodynamics in straight channels rotating relative to a parallel axis or an oblique one (Review), *Teplofiz. Vys. Temp.*, **34**, No. 3, 461–473 (1996).
8. I. V. Shevchuk and A. A. Khalatov, Heat transfer and hydrodynamics in the fields of mass forces: Review of work performed at the Institute of Engineering Thermophysics of the National Academy of Sciences of Ukraine, *Prom. Teplotekh.*, **34**, No. 4, 5–19 (2012).
9. A. V. Sudarev and V. I. Antonovskii, *Combustion Chambers of Gas Turbine Plants: Heat Exchange* [in Russian], Mashinostroenie, Leningrad (1985).
10. A. A. Khalatov, A. A. Avramenko, and I. V. Shevchuk, *Heat Exchange and Hydrodynamics in the Fields of Centrifugal Mass Forces*, in 9 vols., Vol. 4, *Engineering and Technological Equipment* [in Russian], Inst. Tekh. Teplofiz. NAN Ukrainy, Kiev (2000).
11. I. G. Dik and O. V. Matvienko, Some features of the heat exchange in swirling internal flows, *Izv. Sib. Otd. Akad. Nauk SSSR, Ser. Tekh. Nauk*, Issue 3, 40–43 (1989).
12. I. G. Dik and O. V. Matvienko, Heat exchange in swirling flows with a volumetric heat source, *Zh. Prikl. Mekh. Tekh. Fiz.*, No. 5, 113–116 (1989).
13. B. S. Petukhov, L. G. Genin, S. A. Kovalev, and S. L. Solov'ev, *Heat Transfer in Nuclear Power Units* [in Russian], MÉI, Moscow (2003).
14. I. B. Vikhorev, Heat exchange and drag in internal flows of chemically reacting multicomponent gas mixtures, *Vestn. MGTU*, **1**, No. 2, 89–94 (1998).
15. B. S. Petukhov, V. D. Vilenskii, V. K. Shikov, and V. I. Barsukov, Heat transfer in laminar flow of nonequilibrium-dissociating nitrogen dioxide in a circular tube, *Teplofiz. Vys. Temp.*, **11**, No. 2, 342–345 (1973).
16. I. G. Dik and O. V. Matvienko, Heat transfer in chemically reacting swirled flows, *Heat Transf. Res.*, **25**, Issue 4, 511–514 (1993).
17. O. V. Matvienko and A. M. Bubenchikov, Mathematical modeling of the heat transfer and chemical reaction of a swirling flow of a dissociating gas, *J. Eng. Phys. Thermophys.*, **89**, No. 1, 127–134 (2016).
18. Ya. B. Zel'dovich, G. I. Barenblatt, V. B. Librovich, and G. M. Makhviladze, *Mathematical Theory of Combustion and Explosion* [in Russian], Nauka, Moscow (1980).
19. A. H. Lefebvre, *Heat-Transfer Processes in Gas-Turbine Combustion Chambers* [Russian translation], Mir, Moscow (1986).
20. I. G. Dik and O. V. Matvienko, Heat transfer and combustion for a spiral flow in an ideal-displacement reactor, *J. Eng. Phys. Thermophys.*, **60**, No. 2, 171–177 (1991).
21. V. B. Nesterenko and B. E. Tverkovkin, *Heat Transfer in Nuclear Reactors with a Dissociating Heat-Transfer Agent* [in Russian], Nauka i Tekhnika, Minsk (1980).
22. I. G. Dik and O. V. Matvienko, Heat transfer in a swirling flow with an endothermic reaction, *Teplofiz. Vys. Temp.*, **28**, No. 1, 190–191 (1990).
23. V. B. Nesterenko, B. E. Tverkovkin, L. N. Shegidevich, and A. P. Yakushev, Heat and mass transfer during the laminar flow of dissociating N_2O_4 gas in a triangular bundle of cylinders, *J. Eng. Phys. Thermophys.*, **29**, No. 3, 1171–1176 (1975).
24. V. B. Nesterenko, Dissociating nitrogen tetroxide as a promising heat-transfer agent and a working medium of atomic power plants with a gas-cooled fast reactor, *Teploénergetika*, No. 1, 72–78 (1972).
25. V. B. Nesterenko (Ed.), *Physicochemical and Thermophysical Properties of the Chemically Reacting System $N_2O_4 \rightleftharpoons 2NO_2 \rightleftharpoons 2NO + O_2$* [in Russian], Nauka i Tekhnika, Minsk (1976).

26. V. B. Nesterenko, *Physical-Technical Bases of the Application of Dissociating Gases as Heat-Transfer Agents and Working Media in Atomic Power Plants* [in Russian], Nauka i Tekhnika, Minsk (1971).
27. A. K. Krasin, V. B. Nesterenko, N. M. Sinev, V. P. Slizov, V. I. Khorev, B. I. Lomashev, V. P. Bubnov, B. E. Tverkovkin, and V. A. Naumov, Physicochemical bases of the design of a nuclear power plant with a gas-cooled fast reactors and with a dissociating heat-transfer agent (nitrogen tetroxide), *Atom. Énergiya*, **32**, Issue 3, 197–203 (1972).
28. B. S. Petukhov and V. K. Shikov, Heat transfer and drag in the flow of a dissociating nitrogen tetroxide in a pipe. Calculation method. Investigation of a laminar flow, *Teplofiz. Vys. Temp.*, **15**, No. 4, 785–794 (1977).
29. O. V. Matvienko and A. M. Bubenchikov, Mathematical modeling of the heat transfer and chemical reaction of a swirling flow of a dissociative gas, *J. Eng. Phys. Thermophys.*, **89**, No. 1, 127–134 (2016).
30. V. P. Bubnov and V. B. Nesterenko, *Schemes of Conversions of Heat from an Atomic Power Plant Operating on Dissociating Gases* [in Russian], Nauka i Tekhnika, Minsk (1975).
31. V. B. Nesterenko, A. A. Mikhalevich, and B. E. Tverkovkin, *Fast Reactors and Heat-Exchange Apparatuses of an Atomic Power Plant Operating with a Dissociating Heat-Transfer Agent* [in Russian], Nauka i Tekhnika, Minsk (1978).
32. A. A. Mikhalevich, *Nuclear Power Engineering: Prospects for Belarus* [in Russian], Belaruskaya Navuka, Minsk (2011).
33. B. S. Petukhov, *Problems of Heat Exchange* [in Russian], Nauka, Moscow (1987).
34. B. S. Petukhov and V. K. Shikov, Heat exchange and drag in the flow of a dissociating nitrogen tetraoxide in a pipe. Investigation of a turbulent flow, *Teplofiz. Vys. Temp.*, **15**, No. 5, 1034–1046 (1977).
35. V. B. Nesterenko, On the influence of thermal effects of chemical reactions in a dissociating heat-transfer agent on the thermodynamic efficiency of an atomic power plant, *Atom. Énergiya*, **52**, Issue 1, 28–34 (1982).
36. L. G. Loitsyanskii, *Mechanics of Liquids and Gases* [in Russian], Nauka, Moscow (1974).
37. F. R. Menter, Zonal two equation $k-\omega$ turbulence models for aerodynamic flows, *AIAA Paper*, Article 93-2906 (1993).
38. F. R. Menter, M. Kuntz, and R. Langtry, Ten years of industrial experience with the SST turbulence model. Turbulence, in: *Heat and Mass Transfer 4*, Begell House. Inc. (2003), pp. 625–632.
39. P. R. Spalart and M. Shur, On the sensitization of turbulence models to rotation and curvature, *Aerospace Sci. Technol.*, No. 1 (5), 297–302 (1997).
40. P. Bradshaw, D. H. Ferriss, and N. P. Atwell, Calculation of boundary layer development using the turbulent energy equation, *J. Fluid Mech.*, **28**, 593–616 (1967).
41. O. A. Kanishchev and V. G. Konakov, Quantitative estimation of the composition of an amil vapor in the process of its use, *Vestn. SPbGU, Ser. 4*, **2** (60), Issue 1, 98–101 (2015).
42. R. A. Svebla and R. S. Brokaw, *Thermodynamic and Transport Properties for the $N_2O_4 \leftrightarrow 2NO_2 \leftrightarrow 2NO + O_2$ System*, NASA TN D-3327 (1966).
43. O. V. Matvienko, Heat transfer and formation of turbulence in an internal swirling fluid flow at low Reynolds numbers, *J. Eng. Phys. Thermophys.*, **87**, No. 4, 940–950 (2014).
44. S. Patankar, *Numerical Heat Transfer and Fluid Flow* [Russian translation], Énergoatomizdat, Moscow (1983).
45. J. P. Van Doormal and G. D. Raithby, Enhancements of the SIMPLE method for predicting incompressible fluid flows, *Numer. Heat Transf.*, **7**, 147–163 (1984).
46. V. Yu. Petrovich, B. E. Tverkovkin, S. L. Zubtsova, and N. N. Tushin, Investigation of the heat and mass transfer in the turbulent flow of the chemically reacting system $N_2O_4 \rightleftharpoons 2NO_2 \rightleftharpoons 2NO + O_2$ in a heating pipe, in: V. B. Nesterenko (Ed.), *Dissociating Gases as Heat-Transfer Agents and Working Media of Power Plants* [in Russian], Nauka i Tekhnika, Minsk (1976), Part II, pp. 16–32.